POLITECNICO DI TORINO
Repository ISTITUZIONALE

Empirical formulation of the out-of-plane resistance of infilled frames

Original
Empirical formulation of the out-of-plane resistance of infilled frames / Di Trapani, F.; Vizzino, A.; Tomaselli, G.; Shing, P. B.. - ELETTRONICO. - 1:(2021), pp. 955-969. (Intervento presentato al convegno 8th International Conference on Computational Methods in Structural Dynamics and Earthquake Engineering, COMPDYN 2021 tenutosi a grc nel 2021) [10.7712/120121].

Availability:
This version is available at: 11583/2970696 since: 2022-08-20T17:59:36Z

Publisher:
National Technical University of Athens

Published
DOI:10.7712/120121

Terms of use:

This article is made available under terms and conditions as specified in the corresponding bibliographic description in the repository

Publisher copyright

(Article begins on next page)

17 August 2024

COMPDYN 2021
8th ECCOMAS Thematic Conference on
Computational Methods in Structural Dynamics and Earthquake Engineering
M. Papadrakakis, M. Fragiadakis (eds.)
Streamed from Athens, Greece, 27–30 June 2021

EMPIRICAL FORMULATION OF THE OUT-OF-PLANE RESISTANCE OF INFILLED FRAMES

Fabio Di Trapani[1*], Alessandro Vizzino[1], Giovanni Tomaselli[1], P. B. Shing[2]

[1] Politecnico di Torino
Dipartimento di Ingegneria Strutturale Edile e Geotecnica
Corso Duca degli Abruzzi 24
{fabio.ditrapani, giovanni.tomaselli, alessandro.vizzino}@polito.it

[2] University of California San Diego
Dept of structural Engineering
La Jolla, CA 92093
pshing@ucsd.edu

Abstract

The assessment of out-of-plane resistance of infilled frames is an issue of primary importance, in fact, post-earthquake damage observations have shown that infills subject to combined in-plane and out-of-plane inertial forces may fail out-of-plane. This collapse mode results particularly dangerous for the safety of people in the proximity area of a building subject to earthquake loads. Therefore, the possibility to perform accurate safety evaluations is fundamental to prevent this kind of failures. Available expressions for the evaluation of out-of-plane resistance of infilled frames are based on too restricted or too large datasets of experimental investigations. Because of this, such expressions are many times conflicting, showing good reliability in some cases and less in others. In order to fill this gap, this paper proposes a new data-driven empirical expression estimating OOP resistance of infilled frames. This expression is based on hybrid data-set, merging experimental data with data from numerical simulations obtained from a refined FE micro-model. The new expression has the advantage to take into account both the aspect ratio of the infilled frame, the influence of vertical loads and the mode of application of the OOP load*. Validation tests are finally carried out against experimental and numerical specimens.*

Keywords: ABAQUS, empirical, FEM, Masonry, Infilled Frames, Reinforced concrete, Data-driven

1 INTRODUCTION

The evaluation of out-of-plane (OOP) resistance of infilled frames is an issue of primary importance in the assessment of seismic risk of frame structures. In fact, even if infills are not primary structural elements, they strongly interact with primary structures undergoing in-plane (IP) damage and therefore becoming more vulnerable against out-of-plane forces. OOP failure of infills if quite dangerous to the safety of people who are around a building during an earthquake. Simple and at the same time reliable verification methods are therefore necessary to engineers to perform safety checks of OOP resistance of masonry infills.

Experimental and numerical studies have been carried out in recent years to investigate the behaviour of infilled frames subjected to combined in-plane and out-of-plane (IP + OOP) actions [1-8]. These studies converged in claiming that, following a seismic event, infill panels are weakened due to in-plane actions and combined IP and OOP cracks lead to different potential damage, ranging from the loss of functionality of the infill to its complete collapse. It should be also observed that infills with moderate-to-low slenderness and well restrained at the sides, can develop significant resistance and displacement capacity because of the arching mechanism and two-way bending effect which develops under out-of-plane actions. Several studies addressed specifically out-of-plane resisting mechanism [1,4,5,7,9-18], developing different formulations estimating OOP resistance to perform safety checks [1,18-24]. Although starting from similar theoretical consideration, results provided by these models are often conflicting [24], giving the impression that some of them are more reliable in some cases and less in others. The recognized difficulty of analytical models to achieve a general validity is due to three major aspects: a) large heterogeneity masonry constitutive materials and different potential combination with the boundary frames in terms of aspect ratio, slenderness, relative strength and stiffness; b) limited experimental background (e.g. with respect to in-plane tests); c) different OOP test loading condition (e.g. 4-point OOP test or airbag uniform pressure test). Because of these uncertainties, the definition of a generalized relationship providing a good estimation of the OOP resistance of masonry infill is still a needed.

Considering the aforementioned aspects, this paper proposes a new empirical expression estimating OOP resistance of infilled frames. The formulation of the new predictive model is based on a hybrid data-set collecting data from real experimental tests and numerical tests from a refined FE model realized in Abaqus environment which has been experimentally calibrated and validated. Parametric analyses on the FE model were carried out to generate additional reference numerical tests investigating the effect of the variation of mechanical, geometric and load conditions on the ultimate OOP resistance. A reliability comparison with available literature model is finally presented.

2 CONSIDERATIONS ON LITERATURE DESIGN MODELS FOR THE EVALUNATION OF OUT-OF-PLANE RESISTANCE OF MASONRY INFILLS

For the sake of space a selection of only four literature models is presented. To make the different formulations comparable, they are expressed in terms of OOP force, by multiplying the ultimate pressure by the area of the infill (w x h). One of the most popular expressions for the estimation of the ultimate OOP load capacity of an infilled frames (F_{OOP}) was proposed by Angel ,1994 [1] and Abrams et al., 1996 [9].

Those studies evaluated the out-of-plane resistance of masonry infills as a function of the degree of in plane damage. Results brought a formulation able to take in consideration the effect of previous in-plane damage and the effect of frame stiffness according to the following formulation:

$$F_{OOP} = \frac{2 f_m}{(h/t)} \cdot \lambda \cdot R_1 \cdot R_2 \cdot w \cdot h \tag{1}$$

where f_m is the vertical compressive strength of the masonry expressed in [MPa] and h, w and t are the infill height, width and thickness respectively. The lengths are expressed in [mm]. Coefficients R_1, R_2 and λ, are related to the degree of in-plane damage (Eq. 2), to the frame members flexural stiffness (Eq. 3) and to the infill slenderness (Eq. 4) respectively, so that:

$$R_1 = \left(1.08 + \left(\frac{h}{t}\right)\left\{-0.015 + \left(\frac{h}{t}\right)\left[-0.00049 + 0.000013\left(\frac{h}{t}\right)\right]\right\}\right)^{\Delta/2\Delta_{cr}} \tag{2}$$

$$R_2 = 0.357 + 2.49 \times 10^{-14} EI \leq 1.0 \tag{3}$$

$$\lambda = 0.154 e^{-0.0985(h/t)} \tag{4}$$

in which Δ is the current previous in-plane relative displacement, Δ_{cr} is the same displacement associated with the formation of the first crack in the panel, EI is the flexural rigidity of the smallest element composing the concrete frame.

In the Eurocode 6 [22], the following formulation, based on the one-way arching mechanism, is provided:

$$F_{OOP} = f_m \left(\frac{t}{h}\right)^2 \cdot w \cdot h \tag{5}$$

Symbols appearing in Eq. (5) have the same meaning of those previously described. In this formula the out-of-plane resistance has inverse proportionality with the square of the infill slenderness ratio. An adjustment of the prediction models in Eq. (5) has been provided by Ricci et al. 2017 [23], who corrected the expression with the introduction of empirical coefficients. The experimental dataset included the tests by Angel 1994 [1], Flanagan e Bennet 1999 [10,11], Calvi and Bolognini 2001 [12], Hak et al. 2014 [13] and Furtado et al. 2016 [14]. The obtained final formulation was:

$$F_{OOP} = 1.95 f_m^{0.35} \frac{t^{1.59}}{h^{2.96}} \cdot w \cdot h \tag{6}$$

where the lengths are expressed in mm.

More recently, Liberatore et al. 2020 [24] provided a further updated considering also the influence of the aspect ratio (h/l) on the infill with the following expression:

$$F_{OOP} = 0.26 f_m^{0.9} \frac{h}{l}\left(\frac{h}{t}\right)^{-1.23} \cdot w \cdot h \tag{7}$$

Previous studies (e.g. Liberatore et. al 2020 [24]) have shown significant scattering of predictive results from these expressions, but two major considerations have to be done. The first is that some of these expression (e.g. Angel et al. 1994 [1]) were based on a limited experimental dataset. The second is that is it not realistic thinking that these expressions can be reliable in predicting the OOP resistance even of infills with RC of steel frames and also of

confined masonry. Considering single categories would be more proper but, of course, this would reduce the experimental database. The strategy adopted in the following of the paper aims to consider only infills with reinforced concrete frames. A selected number of very complete experimental tests was considered to form the database. The latter is expanded through the definition of a numerical database that is generated based on refined FE model of infilled RC frame, experimentally validated. Details of the model definition are provided in the following section.

3 REFINED FE MICRO-MODEL

The refined FE micro-model was realized with the Abaqus [25] software platform. Masonry blocks constituting the infill were modelled individually as well as frame and reinforcement elements. Mortar joint between blocks and between blocks and columns were modelled by frictional interface elements. The reference experimental test used for the model definition and calibration is specimen 80_OOP_4E by Ricci et al. 2018 [5]. The reference test considers a hollow clay masonry infilled RC frame infill restrained at the four sides having dimensions 2350mm x 1830 mm and thickness 80 mm (Fig. 1a). The out-of-plane load was applied by imposing an out-of-plane displacement with an actuator equipped with four point-load devices (Fig. 1b). Mechanical properties of specimen materials are shown in shown in Table 1.

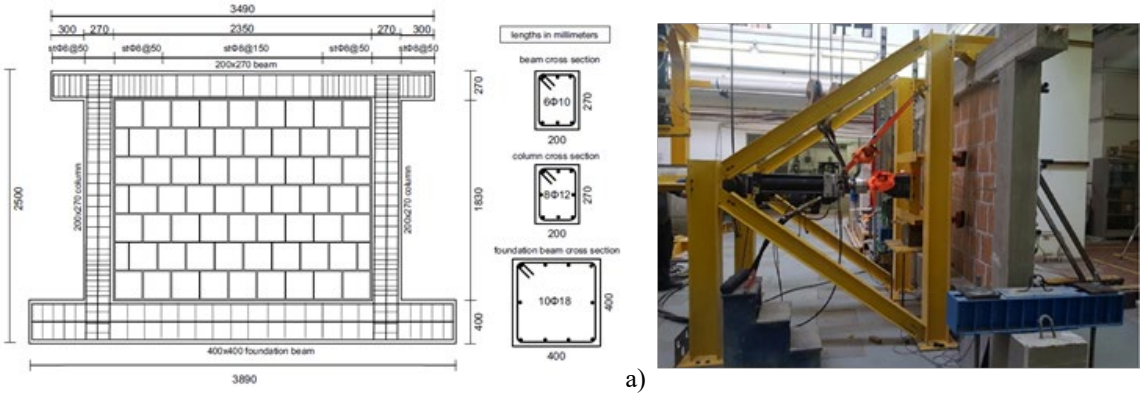

a) b)

Figure 1: Specimen 80_OOP_4E by Ricci et al. 2018 [5]: a) Design details of the specimen; b) Test setup.

Mechanical properties	Symbol	Mean value (MPa)
Concrete compressive strength	f_{cm}	36.00
Steel rebars' yielding stress	f_{ym}	552
Masonry tensile strength	f_t	0.23
Bricks' compressive strength (parallel to holes)	f_{bh}	5.00
Bricks' compressive strength (perpendicular to holes)	f_{bv}	2.00
Mortar compressive strength	f_j	8.29

Table 1: Mechanical properties of the materials used in test 80_OOP_4E, Ricci et al. 2018 [5]

The concrete damaged plasticity model was used model the behaviour of brittle materials, namely concrete frame members and masonry blocks. The blocks were modelled as solid isotropic brick elements. To take into consideration the orthotropic behaviour due to the presence of hollows, a quadratic mean between the two compressive resistance in horizontal and verti-

cal direction of the block was used to define a unique reference conventional resistance value ($\tilde{f}_b$), so that:

$$\tilde{f}_b = \sqrt{f_{bh} \cdot f_{bv}} \tag{7}$$

where f_{bh} is the experimental horizontal compressive resistance of the unit and f_{bv} is the vertical one. The conventional elastic modulus of the blocks was estimated as a function of $\tilde{f}_b$, in analogy of what suggested in Eurocode 6 [22] for masonries, as:

$$\tilde{E}_b = 1000 \cdot \tilde{f}_b \tag{8}$$

The constitutive law used to define the compression behaviour of the block is of the parabolic type with a linear softening branch up to the ultimate strain ε_{cu} [26]. The model proposed by Hsu & Mo 2010 [27] was used to describe the tensile behaviour of the blocks. In Fig. 2 the constitutive laws adopted for the masonry units are shown.

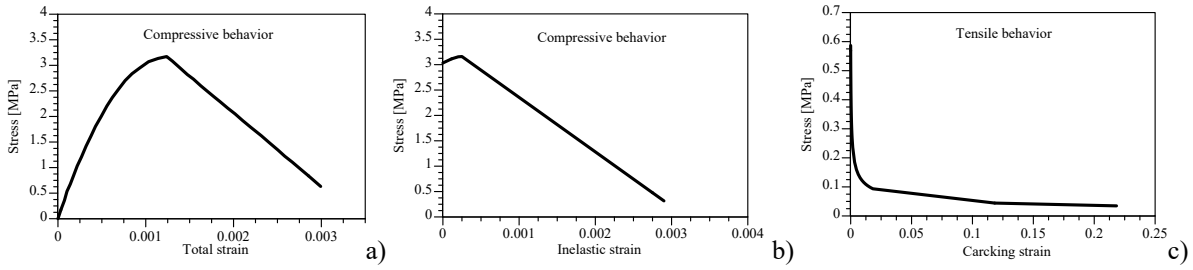

Figure 2: Constitutive laws adopted for masonry blocks: a) Compressive stress- total strain response; b) Compressive stress-inelastic strain response; c)Tensile stress- cracking strain response.

The elastic and plastic parameters in Table 2 are used for the materials definition. As regards the angle of dilatancy for the concrete a value of 37° was assumed as suggested in [25], while for masonry an angle of 10° was adopted as suggested by Van der Pluijm et al. 2000 [28]. Plastic parameters regulating the eccentricity (ε), biaxial resistance domain f_{b0}/f_{co}, and viscosity were assumed as suggested in [25].

Material	Mass density	Elasticity parameters			Plasticity parameters			
	ton/m^3	Young's modulus (MPa)	Poisson's ratio ν	Dilatation Angle ψ	Eccentricity ε	f_{b0}/f_{co}	K_c	*Viscosity*
Concrete	2.5E-09	32308	0.3	37	0.1	1.16	0.667	0.0003
Masonry bricks	1.10E-09	3160	0.2	10	0.1	1.16	0.667	0.0003

Table 2: Material properties of concrete and masonry blocks used in ABAQUS

Steel reinforcement was modelled using 1D truss elements whose mechanical response is simulated by a simple elasto-plastic with strain hardening material model. Steel rebars were modelled as embedded elements within the concrete, so that relative sliding between steel bars and concrete could not occur.

Mortar joints behaviour was modelled using elasto-plastic interfaces with friction and cohesion. The interface normal (k_{nn}) and transverse (k_{ss}, and k_{tt}) stiffnesses were obtained following a calibration process of the model. Obtained values are reported in Table 3.

Tangential	Normal	Stiffnesses (MPa)		
Friction coefficient	Hard contact	K_{nn}	K_{ss}	K_{tt}
0.6		200	88	88

Table 3: Interfaces mechanical properties.

All the model elements were modelled by solid 3D elements with 8 nodes (C3D8R) with a sufficiently refined mesh. Fig. 3 shows the scheme of the model assembly (Fig. 3a) and the mesh of the elements (Fig. 3b). A non-linear quasi-static analysis was performed to simulate the test. Out-of-plane displacements were imposed at the four loading plates.

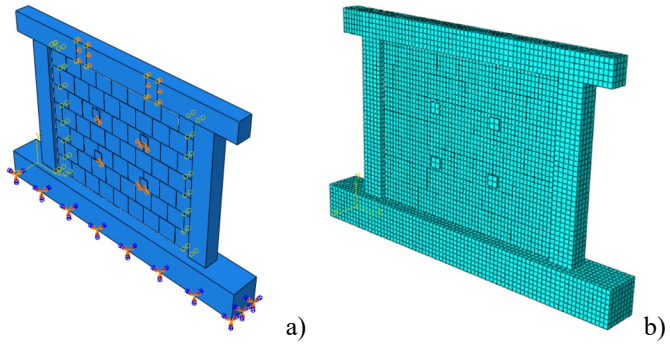

Figure 3: Definition of the micromodel: a) Scheme of the model assembly; b) Mesh of the model,

Results of the numerical simulation of the OOP test are shown in Fig. 4 and compared with the experimental response. It can be observed that the model is able to effectively reproduce the experimental behaviour in terms of initial stiffness, peak resistance, and the post peak behaviour. The deformed shape of the model in correspondence of the peak load is also shown in Fig. 5.

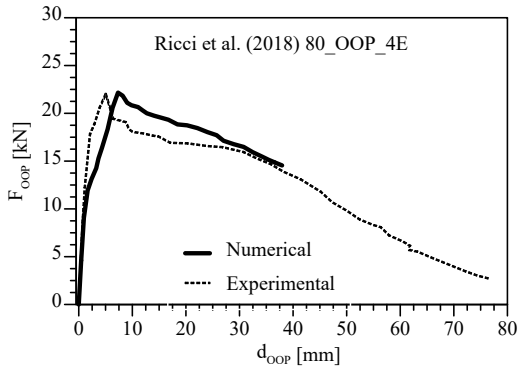

Figure 4: Comparison between numerical simulation and experimental response of the OOP test 4E by Ricci et al. 2018 [5]

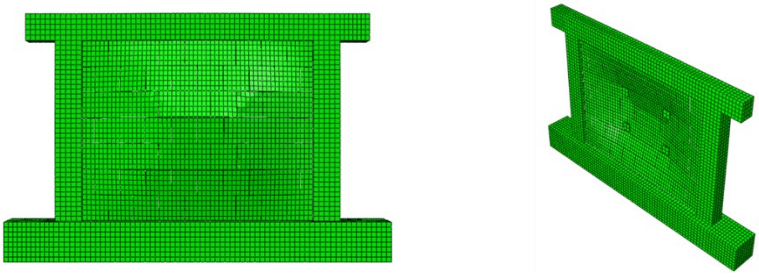

Figure 5: Deformed shape of the infilled frame micro-model in correspondence of the peak-load

The analysis allowed also an investigation in terms of stress distribution and damage localization. Figs. 6-7 show the compressive and tensile principal stresses on the windward and leeward sides of the specimen in correspondence of the peak load. The analysis of the stress filed confirms that the model effectively reproduced the horizontal and vertical arching action and the 2-way bending response. A further comparison between tensile damage pattern resulting by the FE model at the ultimate displacement and real cracking pattern in shown in Fig. 8, confirming a certain consistency.

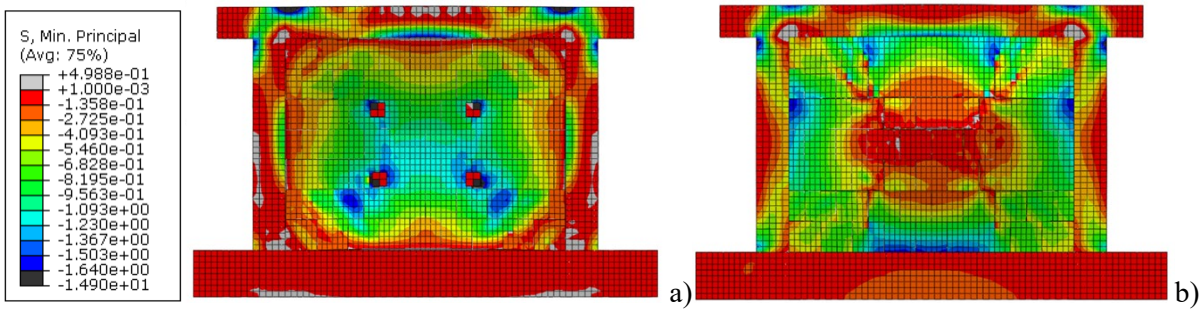

Figure 6: Compressive stress field at the peak load: a) windward side; b) leeward side.

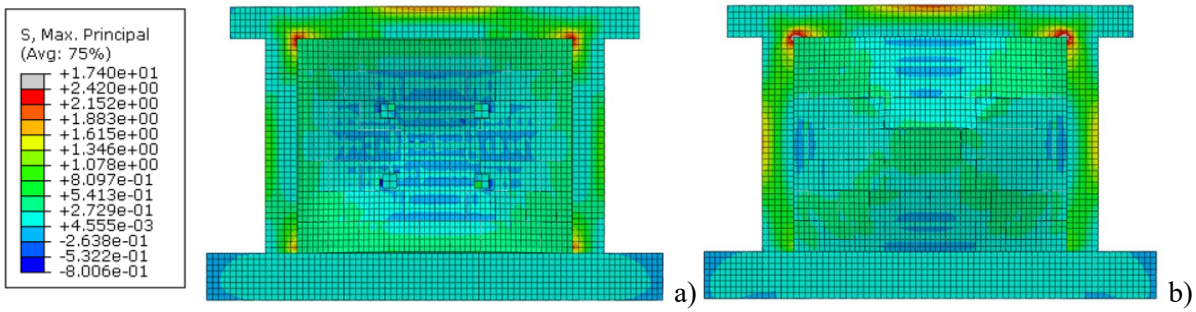

Figure 7: Tensile stress field at the peak load: a) windward side; b) leeward side.

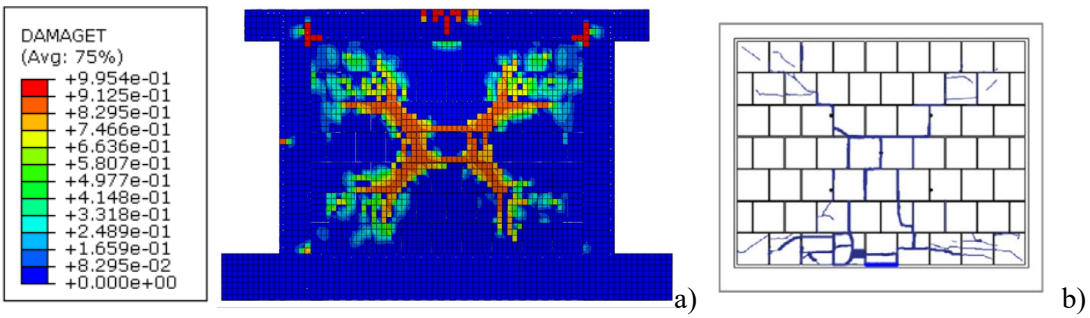

Figure 8: Ultimate displacement damage at: a) model tensile damage pattern; b) experimental cracking pattern by Ricci et. al 2018 [5].

After the calibration, the model predictive capacity has been blind-tested against two further experimental tests. These were specimens 120_OOP_4E by Ricci et al. 2018 [5] and De Risi et al. 2019 [7]. These two specimens were modelled according to the above described procedure. Experimental / numerical comparisons are shown in Fig. 9. The latter, besides validating the model, confirmed its suitability to be used as a reliable predictive tool to generate reliable simulated tests.

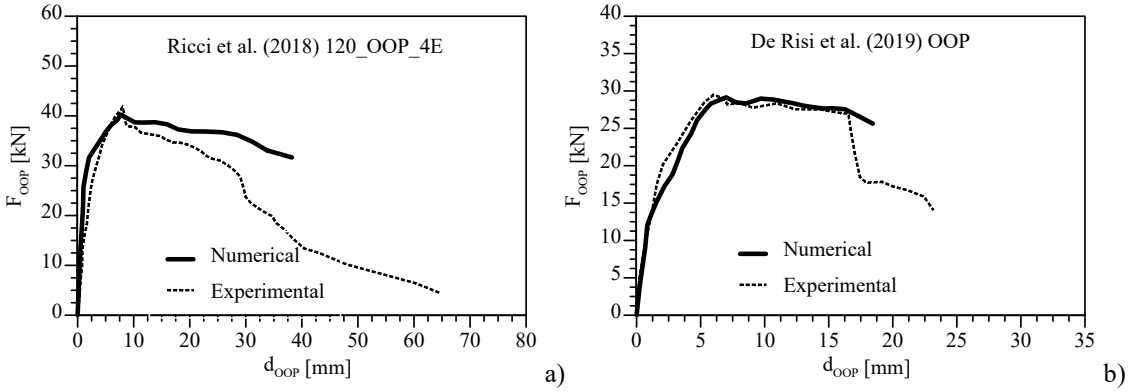

Figure 9: Comparison of numerical and experimental OOP response: a) Specimen 120_OOP_4E by Ricci et al. 2018 [5]; (b) Specimen by De Risi et al. 2019 [7] OOP

4 PARAMETRIC INVESTIGATION

The additional FE tests were generated starting from the reference models and individually varying single parameters. In this way, the influence of each variation to the overall resistance was analysed. Varied parameters were the infill slenderness (h/t), the blocks conventional resistance ($\tilde{f}_b$), the entity of the distributed load applied on the upper beam (q).

The variation of the slenderness ratio was performed on two different models, characterized by a different aspect ratio (w/h=1-1.28). The slenderness was varied between 9.15 and 22.87, to cover a sufficiently wide range. Results confirmed inverse proportionality between OOP ultimate load and slenderness (Figs. 10-11).

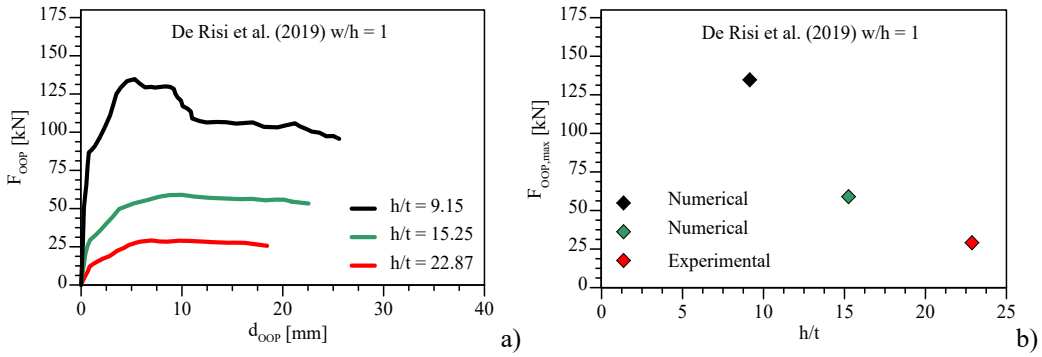

Figure 10: Effect of slenderness variation (w/h = 1.00): a) OOP force-displacement curves; b) Maximum OOP force vs. slenderness.

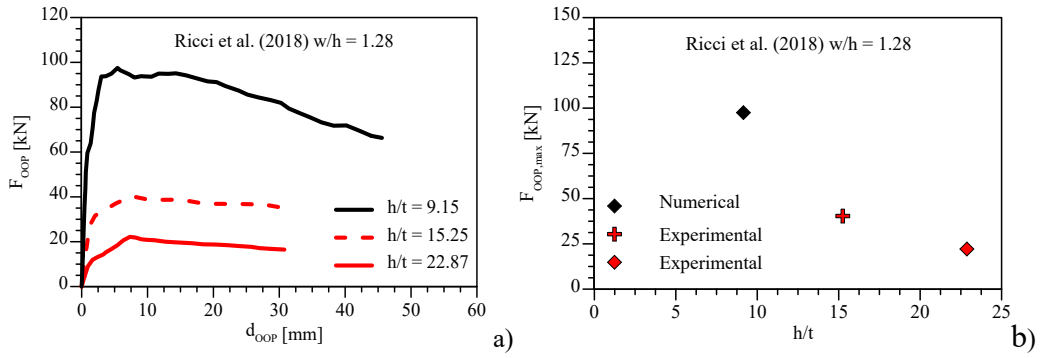

Figure 11: Effect of slenderness variation (w/h = 1.28): a) OOP force-displacement curves; b) Maximum OOP force vs. slenderness.

The effect of units resistance variation was evaluated on three different models, Ricci et al. 2018 [5] (infill thickness 80 and 120 mm) and De Risi et al. 2019 [7]. The latter was varied in the range 0.5-2.0 $\tilde{f}_{b,ref}$, where $\tilde{f}_{b,ref}$ is the conventional resistance originally used in the calibration and validation phases. Results show that an increment of the unit strength involves an increase of the out-of-plane resistance of the infilled frame (Figs. 12-14). This behaviour seems to be characterized by a limit, beyond which further increases of the unit strength do significantly affect the OOP resistance.

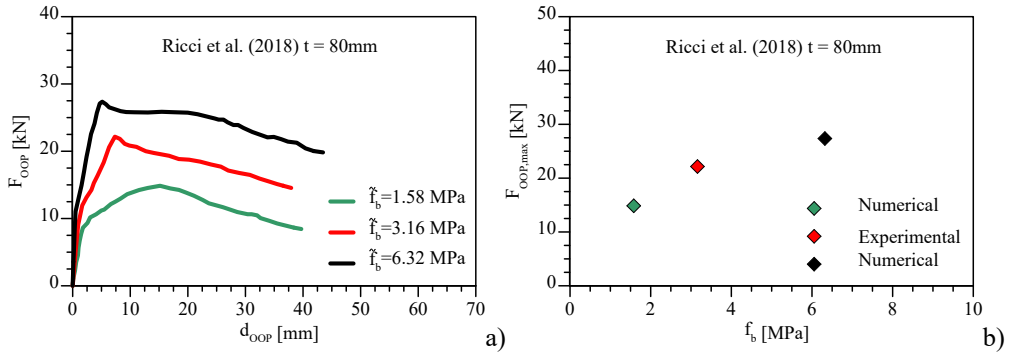

Figure 12: Effect of unit's compressive strength on the ultimate OOP capacity: a) OOP force-displacement curves; b) Maximum OOP force vs. $\tilde{f}_b$. Reference specimen by Ricci et al. 2018 (t=80 mm) [5]

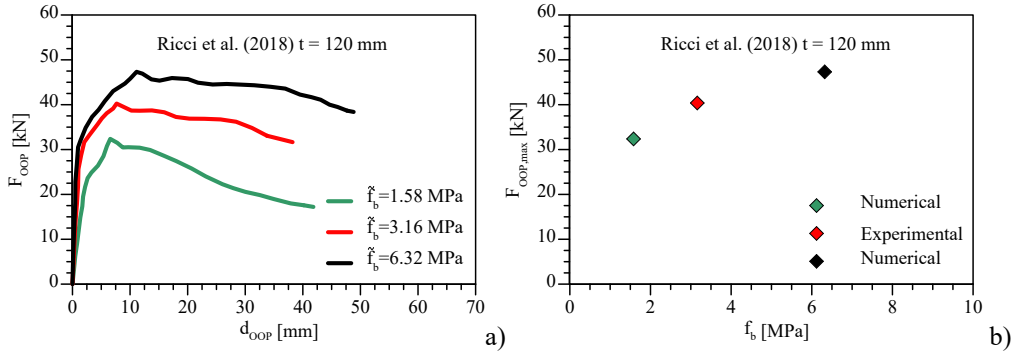

Figure 13: Effect of unit's compressive strength on the ultimate OOP capacity. a) OOP force-displacement curves; b) Maximum OOP force vs. $\tilde{f}_b$. Reference specimen in Ricci et al. 2018(t=120 mm) [5]

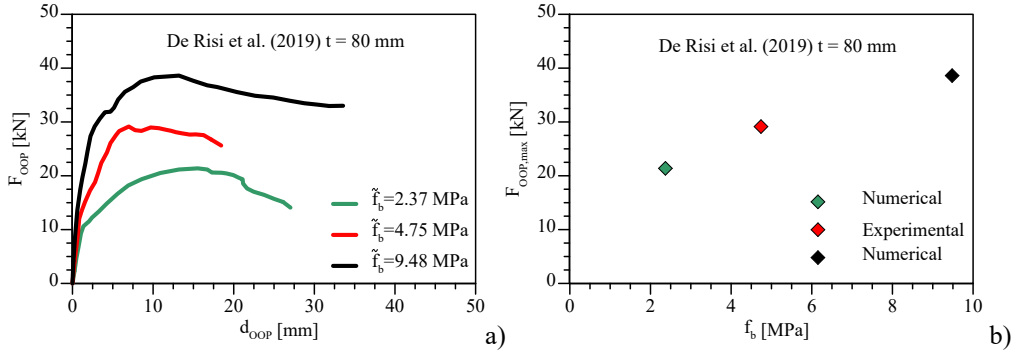

Figure 14: Effect of unit's compressive strength on the ultimate OOP capacity. a) OOP force-displacement curves; b) Maximum OOP force vs. $\tilde{f}_b$. Reference specimen in De Risi et al. 2019 (t=80 mm) [7]

The influence of a distributed load acting on the top beam was finally investigated using specimen 80_OOP_4E [5] as reference. The load was varied in the range 0-30 kN/m.

A linear increment of the OOP resistance was observed as a function of the extent of the vertical load (Fig. 15). This trend is justified by the pre-stressing action exerted on the infill by the compression load, which makes the arching mechanism more effective.

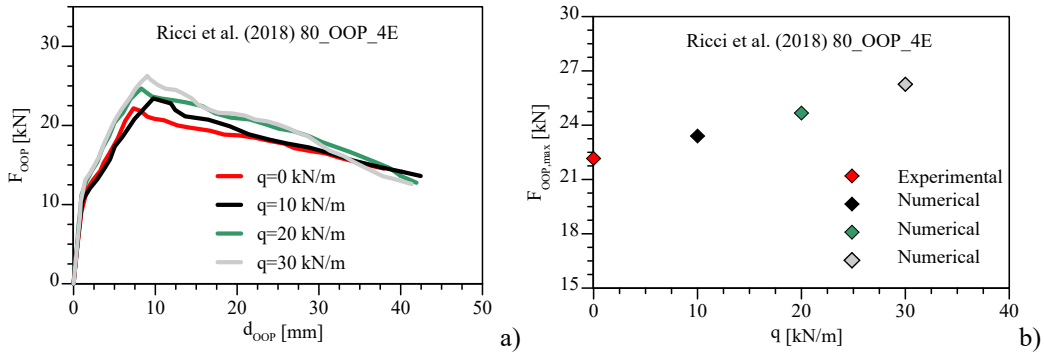

Figure 15: Effect of vertical load (q) on the ultimate OOP capacity. a) OOP force-displacement curves; b) Maximum OOP force vs. q. Reference specimen in Ricci et al. 2018 (t=80 mm) [5]

5 DEFINITION OF THE EMPIRICAL FORMULATION

An hybrid database composed of 9 experimental tests [1,4,5,7,12,15-17] and the 13 numerical simulations presented before was assembled to put in relation test results with the geometric and mechanical properties of the infilled frames. Data processing was performed to derive an empirical analytical relationship between the out-of-plane resistance the most relevant geometric and mechanical features of a generic infilled RC frame. The reference experimental tests and the numerical simulations are collected in Tab. 4 together with the specification of the parameters varied for each test/simulation and the modality of application of the vertical load. This latter parameter has been specifically investigated to evaluate its influence in conditioning the out-of-plane resistance. To highlight this aspect a specific test was carried out using the reference FE model 8_OOP_4E [8] and simulating its OOP response by applying a uniform load (instead of the original 4-point loading), which is more similar to the actual trend of inertial forces. Results evidenced a double OOP resistance if the infill is uniformly loaded (Fig. 16).

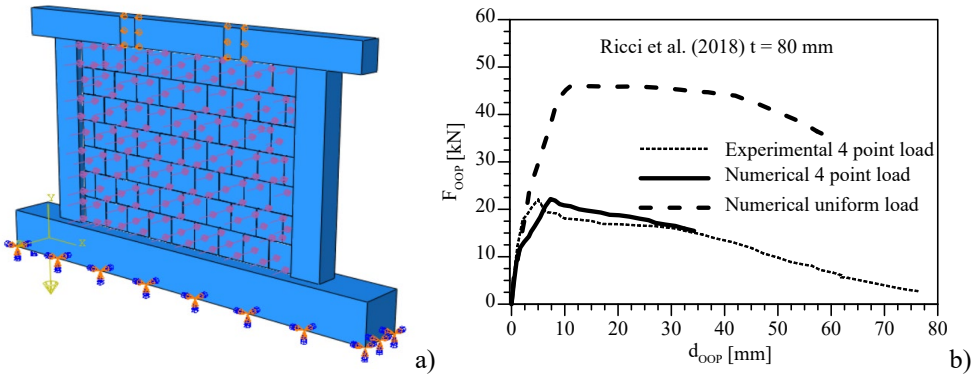

Figure 16: Effect of the way of application of the OOP load on the ultimate capacity: a) Simulation of the application of the uniform load on the FE model; b) OOP response of the FE model with 4-point and uniform load.

In consideration of results of previous numerical tests and past experimental evidence the search for a new empirical formulation considered the following major parameters: aspect ratio of the infill (w/h), slenderness of the infill (h/t), conventional resistance of the units ($\tilde{f}_b$),

resulting vertical load acting on the upper beam ($Q = q \cdot w$) and mode of application of the OOP load (α). The latter coefficient allows uniformizing OOP test results obtained by 4-point load tests and airbag tests (uniform loading). The proposed predictive relationships allows direct evaluation of the undamaged OOP resistance of an infilled frame. The latter has the following expression:

$$F_{OOP} = \alpha \cdot \left[\left(\frac{w \cdot h}{100} \right)^{\beta} \left(\frac{w}{h} \right)^{-0.41} \tilde{f}_b^{0.43} \left(\frac{h}{t} \right)^{-1.67} + 0.058 \cdot Q \right] \tag{9}$$

where β is an aspect-ratio related coefficient defined as:

$$\beta = -0.372 \cdot \left(\frac{w}{h} \right)^2 + 0.787 \frac{w}{h} + 0.3455 \tag{10}$$

and α is the conversion factor used to make experimental 4-point load test and uniform load tests comparable and assuming the following values:

$$\begin{cases} \alpha = 1 & 4-\text{point load} \\ \alpha = 1.557 \left(\frac{w}{h} \right)^{1.138} & \text{uniform load} \end{cases} \tag{11}$$

A comparison between experimental and numerical OOP resistance values with the predictions by Eq. (9) is shown in Fig. 17, demonstrating very low dispersion of results by the proposed empirical model.

Test reference	Specimen	h (mm)	w (-)	w/h (mm)	t (mm)	h/t (-)	$\tilde{f}_b$ (N/mm^2)	Q (kN)	Load appl.	F_{OOP} (kN)
Ricci et al. [5]	80_OOP_4E	1830	2350	1.28	80	22.9	3.16	0	4-point	22.16
	120_OOP_4E	1830	2350	1.28	120	15.3	3.16	0	4-point	41.90
De Risi et al. [7]	OOP	1830	1830	1.00	80	22.9	4.74	0	4-point	29.14
Calvi & Bolognini [12]	10	2750	4200	1.53	135	20.4	6.57	0	4-point	33.70
Koutas & Bournas [16]	S_CON	1250	1700	1.36	65	19.2	21.00	0	4-point	29.00
Angel et al. [1]	1	1625	2438	1.50	48	33.9	23.90	0	Airbag	33.90
Sepasdar [4]	IF-ND	980	1350	1.38	90	10.9	12.80	0	Airbag	87.71
Akhoundi et al. [15]	SIF-B	1635	2415	1.48	80	20.4	4.29	0	Airbag	39.70
Nasiri & Liu [17]	IFNG	980	1350	1.38	90	10.9	25.00	0	Airbag	140.00
FEM – Analyses	FEM-R-L1	1830	2350	1.28	80	22.9	3.16	0	Airbag	45.43
	FEM-DR-G1	1830	1830	1.00	120	15.3	4.74	0	4-point	56.98
	FEM-R-G2	1830	2350	1.28	200	9.2	3.16	0	4-point	101.39
	FEM-DR-G2	1830	1830	1.00	200	9.2	4.74	0	4-point	133.72
	FEM-R-M1	1830	2350	1.28	80	22.9	1.58	0	4-point	16.29
	FEM-R-M2	1830	2350	1.28	80	22.9	6.32	0	4-point	29.57
	FEM-DR-M1	1830	1830	1.00	80	22.9	2.37	0	4-point	21.49
	FEM-DR-M2	1830	1830	1.00	80	22.9	9.48	0	4-point	39.00
	FEM-R-M3	1830	2350	1.28	120	15.3	1.58	0	4-point	32.07
	FEM-R-M4	1830	2350	1.28	120	15.3	6.32	0	4-point	58.20
	FEM-R-Q1	1830	2350	1.28	80	22.9	3.16	23.5	4-point	23.31
	FEM-R-Q2	1830	2350	1.28	80	22.9	3.16	47.0	4-point	24.68
	FEM-R-Q3	1830	2350	1.28	80	22.9	3.16	70.5	4-point	26.04

Table 4: Hybrid experimental/numerical database

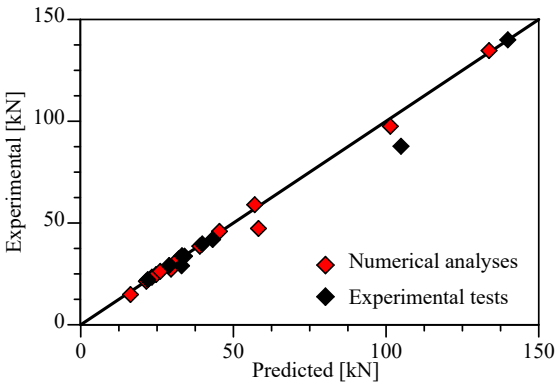

Figure 17: Comparison between experimental and predicted OOP resistance values by the proposed formulation.

6 COMPARISONS WITH THE EXISTING PREDICTIVE MODELS

A comparative analysis of the proposed relationship with respect to the predictive models available in the literature is finally carried. For this comparison only experimental test results were considered. The reference experimental tests and the respective experimental and predicted OOP resistance values are shown Table 5. Results are graphically represented in Fig. 18. It can be observed how the proposed model is able to fit better than the other predictive models. The models proposed by Ricci et al. 2017 [23] and Liberatore et al. 2020 [24] provided also an adequate reliability although they seem having an overestimation tendency. On the contrary, the model by Angel 1994 [1] significantly underestimated the experimental results. The improved predictive capacity shown by the proposed model with respect to the previous ones is justified by the fact that this model enriches the formulation taking into account additional information such as the influence of vertical loads and the mode of application of the out-of-plane load. Moreover, the model is specifically calibrated using only OOP tests of infilled RC frames, therefore it results more accurate than the other formulations base on a more heterogeneous database.

Experimental study	Specimen	$F_{OOP,exp}$ [kN]	$F_{OOP,pred}$ [kN]				
			Angel [1]	EC6 [22]	Ricci [23]	Liberatore [24]	**Proposed model**
Ricci et al. [5]	80_OOP_4E	22.16	6.84	14.88	31.10	52.58	**21.95**
	120_OOP_4E	41.90	19.81	30.51	57.37	31.61	**43.20**
De Risi et al. [7]	OOP	29.14	7.13	15.17	26.62	47.88	**28.95**
Calvi & Bolognini [12]	10	33.70	21.79	30.62	48.30	82.71	**33.99**
Koutas & Bournas [16]	S_CON	29.00	20.95	55.74	61.44	40.28	**33.03**
Angel et al. [1]	1	33.90	10.32	39.12	34.07	16.99	**33.15**
Sepasdar [4]	IF-ND	87.71	47.40	104.89	130.44	170.46	**104.88**
Akhoundi et al. [15]	SIF-B	39.70	3.20	9.45	32.39	80.52	**39.80**
Nasiri & Liu [17]	IFNG	140.00	91.42	190.80	160.83	99.48	**139.87**
		Mean exp/pred	3.49	1.45	0.83	0.86	**0.97**
		Std. Dev.	3.47	1.12	0.24	0.58	**0.07**

Table 5: Experimental OOP resistance values and their analytical prediction.

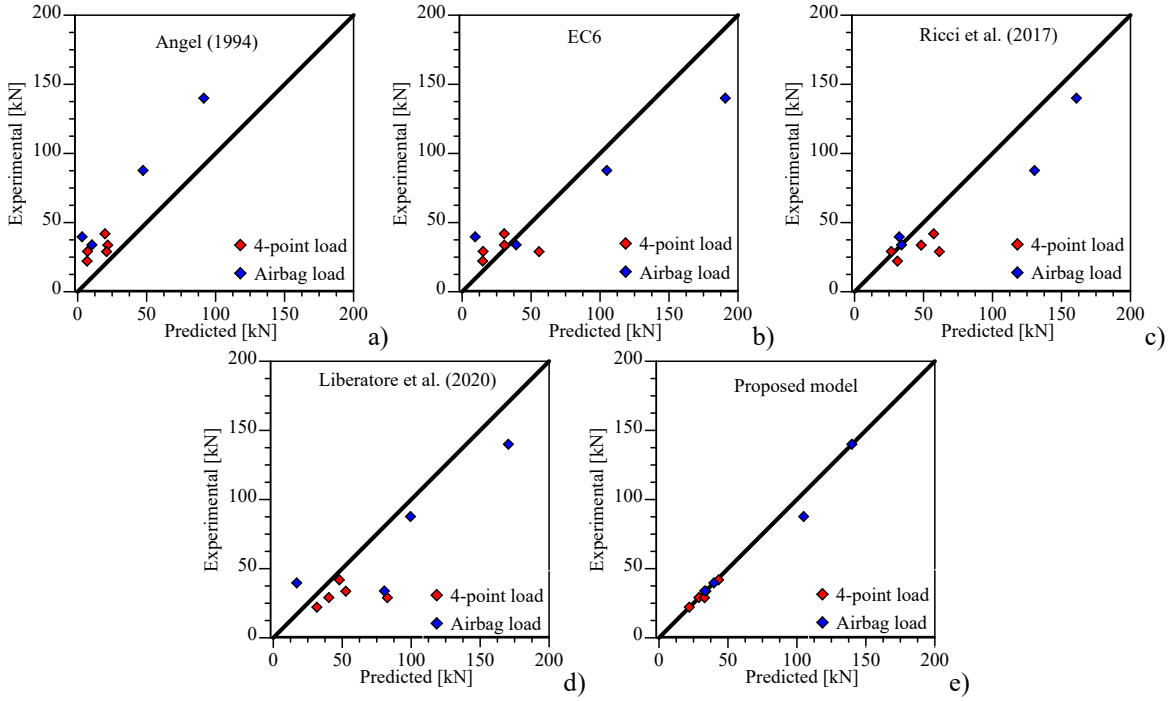

Figure 18: Reliability comparison of models for the prediction of OOP resistance: a) Angel 1994 [1]; b) Eurocode 6 [22]; c) Ricci et al. 2017 [23]; d) Liberatore et al. 2020 [24]; e) proposed model.

7 CONCLUSIONS

Assessment of out-of-plane capacity of infilled frames is not straightforward. Available literature models for the prediction of the out-of-plane resistance are often conflicting, being in general too conservative or, on the contrary, overestimating the capacity. The reasons of this inconsistencies are different. First of all, some of the available models (e.g. Angel et al. [1]) are calibrated based on a limited investigation. Conversely, other literature models have been defined using a too wide dataset, including also steel infilled frames or confined masonries. Finally, the way of application of the OOP load influences on the OOP capacity, therefore some formulations can result unsuitable in match experimental results of specimens loaded with different modalities (e.g. 4-point load or uniform load). In consideration of this, a hybrid database, composed of 9 experimental tests and 13 numerical simulations by a refined FE micro-model was specifically defined. FE models allowed increasing the extent of the dataset and to investigate on the influence of some parameters not taken into account by previous experimental investigations (e.g. the influence of distributed load on the upper beams or the influence of the modality of application of the OOP load).

Postprocessing of the collected data allowed defining a new empirical relationship for the direct estimation of the OOP resistance of a generic infilled frame. The proposed model showed matching better the other the experimental results. The reasons of its better capability in estimating experimental results is justified by the following major considerations:

- The model takes into account the way of application of the OOP load, which greatly influences the OOP resistance.
- The model considers the influence of vertical loads which increase the effectiveness of the arching mechanism.

- The model proposes the use of the conventional unit compressive strength ($\tilde{f}_b$) instead of the vertical strength of the masonry as parameter having major correlation with the OOP resistance of the infill.

REFERENCES

[1] Angel R. Behavior of reinforced concrete frames with masonry infill walls. *University of Illinois at Urbana-Champaign,* Illinois; 1994.

[2] Calvi G.M., Bolognini D. Seismic response of reinforced concrete frames infilled with weakly reinforced masonry panels. *Journal of Earthquake Engineering*, 5, 153-185; 2001.

[3] Morandi P., Hak S., Magenes G. 2011. Report of the experimental campaign on robust clay masonry infills. *Fondazione Eucentre,* Pavia; 2011.

[4] Sepasdar R. Experimental investigation on the out-of-plane behaviour of concrete masonry infilled frames. *Master's Thesis, Dalhousie University*; 2017.

[5] Ricci P., Di Domenico M., Verderame G.M. Experimental assessment of the in-plane/out-of-plane interaction in unreinforced masonry infill walls. *Engineering Structures*, 173, 960–978; 2018.

[6] Wang C. Experimental investigation on the out-of-plane behaviour of concrete masonry infilled frames. *Master's Thesis, Dalhousie University*; 2019.

[7] De Risi M.T., Di Domenico M., Ricci P., Verderame G.M., Manfredi G. Experimental investigation on the influence of the aspect ratio on the in-plane/out-of-plane interaction for masonry infills in RC frames. *Engineering Structures*, 189, 523-540; 2019.

[8] Di Domenico M., De Risi M.T., Ricci P., Verderame G.M., Manfredi G. Empirical prediction of the in-plane/out-of-plane interaction effects in clay brick unreinforced masonry infill walls. *Engineering Structures*, 227, 111438; 2021.

[9] Abrams D.P., Angel R., Uzarski J. Out-of-plane strength of unreinforced masonry infill panels. *Earthquake Spectra*, 12(4), 825–844; 1996.

[10] Flanagan R.D., Bennett R.M. Arching of masonry infilled frames: Comparison of analytical methods. *Practice Periodical on Structural Design and Construction*, 4(3), 105-110; 1999a.

[11] Flanagan R.D., Bennett R.M. Bidirectional behavior of structural clay tile infilled frames. *ASCE Journal of Structural Engineering*, 125(3), 236-244; 1999b.

[12] Calvi G.M., Bolognini D. Seismic Response of Reinforced Concrete Frames Infilled with Weakly Reinforced Masonry Panels. *Journal of Earthquake Engineering*, 5, 153-185; 2001.

[13] Hak S., Morandi P., Magenes G. Out-of-plane experimental response of strong masonry infills. *2nd European conference on earthquake engineering and seismology*; 2014.

[14] Furtado A., Rodrigues H., Arede A., Varum H. Experimental evaluation of out-of-plane capacity of masonry infill walls. *Engineering Structures*, 111, 48-63; 2016.

[15] Akhoundi F., Vasconcelos G., Lourenço P. Experimental out-of-plane behavior of brick masonry infilled frames. *International Journal of Architectural Heritage*, 18, 1-7; 2018.

[16] Koutas L.N., Bournas D.A. Out-of-plane strengthening of masonry-infilled RC frames with textile-reinforced mortar jackets. *Journal of Composites for Construction*, 23 (1); 2019.

[17] Nasiri E., Liu Y. Effect of prior in-plane damage on the out-of-plane performance of concrete masonry infills. *Engineering Structures*, 222, 111-149; 2020.

[18] McDowell E.L., Mckee K.E., Sevin E. Arching action theory of masonry walls. *Journal of the Structural Division*, 82, 915/1-18; 1956a.

[19] Dawe J.L., Seah C.K. Out-of-plane resistance of concrete masonry infilled panels. *Canadian Journal of Civil Engineering*, 16(6), 854-864; 1989.

[20] Bashandy T., Rubiano N., Klingner R. Evaluation and analytical verification of infilled frame test data. P.M. Ferguson Structural Engineering Laboratory, *Report No.95-1, Department of Civil Engineering University of Texas at Austin*, Austin, Tx; 1995.

[21] FEMA 356 (Federal Emergency Management Agency). Prestandard and commentary for the seismic rehabilitation of buildings. *Washington DC: FEMA*; 1997.

[22] CEN (European Committee for Standardisation). Eurocode 6 – Design of masonry structures, Part 1-1: Common rules for reinforced and unreinforced masonry structures. *EN 1996-1-1*, Brussel, Belgium: CEN; 2005.

[23] Ricci P., Di Domenico M., Verderame G.M. Empirical based out of plane URM infill wall model accounting for the interaction with in plane demand. *Earthquake Engng Struct Dyn*;1–26; 2017.

[24] Liberatore L., AlShawa O., Marson C., Pasca M., Sorrentino L. Out-of-plane capacity equations for masonry infill walls accounting for openings and boundary conditions. *Engineering Structures*, 207, 110198; 2020.

[25] Simulia. ABAQUS/CAE *User Manual, version 6.13*; 2013.

[26] Kent D.C., Park R. Flexural Members with Confined Concrete. *Journal of Structural Division*, 97, 1969-1990; 1971.

[27] Hsu T.T.C, Mo Y.L. Unified Theory of Concrete Structures. *John Wiley&Sons*, *Ltd*; 2010.

[28] Van der Pluijm R., Rutten H., Ceelen M. Shear behaviour of bed joints. *12th international brick/block masonry conference,* 1849-1862; 2000.